Laser-generated toroidal helium plasmas

Kooij, V.L.

Citation

Kooij, V. L. (2021, April 28). *Laser-generated toroidal helium plasmas*. *Casimir PhD Series*.
Retrieved from https://hdl.handle.net/1887/3161377

Cover Page

Universiteit Leiden

The handle http://hdl.handle.net/1887/3161377 holds various files of this Leiden University dissertation.

Author: Kooij, V.L.
Title: Laser-generated toroidal helium plasmas
Issue date: 2021-04-28

3
Shocks and successive laser pulse experiments

In our studies on laser-generated, atmospheric pressure, transient toroidal helium plasmas, the low density cavity generated by the laser-induced breakdown plasma proved pivotal. Here, we present a novel technique whereby a second laser-induced breakdown plasma is used as a probe, to directly visualise the propagation of the shock generated by the principal breakdown plasma, and to confirm the existence of the low density cavity formed in its wake. In high-speed Schlieren images, we observe a Mach reflection of shocks, formed by the two-lobe plasma kernel of the principal breakdown plasma, whose enhanced strength is linked to the asymmetrical fluid flow necessary for the development of a toroidal plasma.

3.1 Introduction

In our studies on the development of toroidal helium plasmas generated by a single laser-induced breakdown plasma, the low density cavity generated by this breakdown plasma turned out to be a pivotal element. The existence of this cavity has been made plausible by our model presented in section 2.5, which provided a characteristic time scale at which structure is expected to develop, and in the same section, albeit indirectly, by measurements of the density of helium atoms in the centre of the toroidal plasma.

The repletion of the low density cavity plays a formative role, and we observed that a slight asymmetry in the plasma kernel results in a slightly imbalanced fluid flow along the symmetry axis. However, it remained unanswered why the symmetry of the fluid flow necessary for the development of a toroidal plasma, is so severely broken.

In this chapter we present two methods that have been used to directly visualise the low density cavity. In addition to standard high-speed Schlieren imaging,[1] we visualise the propagation of the shock

[1] Settles 2001.

generated by the principal breakdown plasma, and confirm the existence of the low density cavity formed in its wake, using a novel technique whereby a second laser-induced breakdown plasma has been used as a probe. This successive breakdown plasma has been generated by a second high power Nd:YAG laser.

In the presented high-speed Schlieren images, we observe a Mach reflection of shocks, formed by the two-lobe plasma kernel of the principal breakdown plasma, and link the enhanced strength of Mach reflections to the asymmetrical fluid flow necessary for the development and successive splitting of the toroidal plasmas.

3.2   *Shocks and successive laser pulse experiments*

In figure 3.1 we present images that have been obtained using the aforementioned technique whereby a second laser-induced breakdown plasma is used as a probe. At the time of interest, and delayed with respect to the principal breakdown laser pulse, a second breakdown plasma is created by a second high power Nd:YAG laser. The creation and subsequent evolution of this plasma is highly sensitive to the local number density, which is dictated by the principal breakdown plasma. Plasma creation is even completely suppressed in regions of low density. In figure 3.1, at zero delay, both breakdown plasmas can be observed simultaneously. When the delay is increased, the edge of the low density
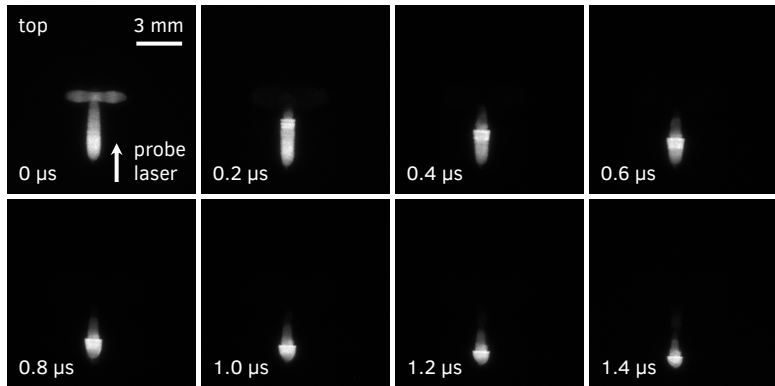

Figure 3.1: Propagation of a shock generated by a laser-induced breakdown plasma, visualised using a second laser-induced breakdown plasma as a probe. The top view images have been captured at increasing times after the principal breakdown laser pulse. Simultaneously, a second breakdown plasma has been created to visualise the shock, which manifests itself in the sharp and clear edge visible in the second breakdown plasma. Note that at 0 µs both the principal and second breakdown plasmas are visible. The images have been individually normalised to their maximum intensity. Principal laser pulse energy: 275 mJ, focal length focussing lens: 50 mm, helium gas pressure: 1000 mbar, bandpass filter: none, ICCD camera image averaging: 10, ICCD camera gate width: 2 ns.

cavity, which manifests itself in the sharp and clear edge visible in the second breakdown plasma, propagates in the subsequent images.

In the presented images, the second breakdown plasma has been created at a distance to the principal breakdown plasma, but when the second plasma would have been created at the same position as the principal plasma, it is completely suppressed for a range of delays. This suppression was already observed during the density measurements presented in section 2.5, and is likewise reported in the literature.[2]

The propagating shock generated by a laser-induced breakdown plasma resembles the blast wave generated by a nuclear explosion,[3] and is likewise observed in supernova remnants.[4] Basic blast wave theory was independently proposed by Taylor, Von Neumann, and Sedov,[5] and assumes an instantaneous energy release into an infinitesimally small volume. Following the energy release, the motion of the shock is described by a power-law time dependence, which for spherical symmetry takes the form of a $t^{0.4}$ dependence.[6]

In figure 3.2 we present the position of the propagating shock that has been visualised in figure 3.1, together with its shock Mach number. The position of the shock has been fitted against a power-law and shows that

[2] Bak, Im et al. 2014; Bak, Wermer et al. 2015.

[3] G. I. Taylor 1950a; G. I. Taylor 1950b; Bethe et al. 1958.

[4] Shu 1992, p. 230; Cioffi 1990.

[5] G. I. Taylor 1950a; Bethe et al. 1958; Sedov 1959.

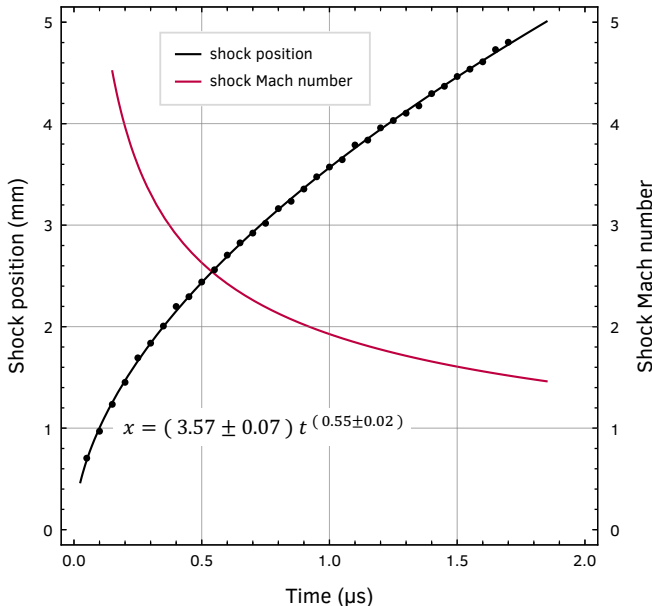[6] Sedov 1959, p. 213; Zel'dovich et al. 1966, p. 93; G. I. Taylor 1950a.

Figure 3.2: Shock position and shock Mach number derived from the visualised shock propagation presented in figure 3.1. The shock position (black dots) has been fitted against a power-law function (black line) and the shock Mach number (purple line) has been obtained by differentiation of the fitted shock position. The speed of sound in the present experimental setting is approximately 1020 m/s.

[7] Sedov 1959, p. 213.

the shock propagates with an exponent of 0.55 ± 0.02. The discrepancy with blast wave theory can be explained from the observation that our plasma kernel exhibits a two-lobe structure, which rudimentary can be seen as a two-dimensional explosion, where a $t^{0.5}$ dependence is expected.[7] Moreover, blast wave theory assumes an instantaneous energy release and neglects internal heat transfer phenomena, including radiation and ionisation, both of which require more sophisticated

[8] Cristoforetti et al. 2006.

models.[8] Earlier studies reported a time dependence of $t^{0.6}$ during the interval between breakdown and the end of the laser pulse,[9] and a

[9] Bradley et al. 2004.

t^1 dependence can be observed during the free expansion phase of a supernova remnant.[10] If we interpret our $t^{0.55}$ dependence as the

[10] Cioffi 1990.

signature of a driven and reinforced shock, the relaxation of meta-stable helium atoms might be the source of the driving energy.

The shock Mach number presented in figure 3.2 has been obtained by differentiation of the fitted shock position, and during the early expansion speeds of up to Mach 4 can be observed. The speed of sound in the present experimental setting is approximately 1020 m/s. When the shock Mach number becomes equal to one, this marks the end of

[11] Zel'dovich et al. 1966.

the shock expansion, and the shock proceeds at sonic speeds.[11] For the shock Mach number presented in figure 3.2 this occurs at 4.3 µs, which qualitatively matches the characteristic time scale of 6.7 µs found using our model presented in section 2.5.

Similar to the method used to visualise the propagating shock, we can visualise the entire shock by sweeping the second breakdown plasma through the low density cavity at a fixed delay. In figure 3.3 we present
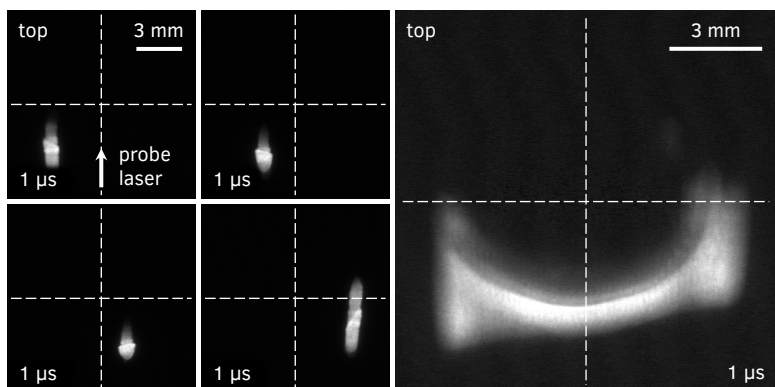

Figure 3.3: Shock generated by a laser-induced breakdown plasma visualised using a second laser-induced breakdown plasma as a probe. (left quartet) The top view images have been captured 1 µs after the principal breakdown laser pulse while sweeping the second breakdown plasma through the shock. (right) The entire shock has been visualised by combining all captured images. The images have been individually normalised to their maximum intensity and are based on recordings captured using identical experimental settings as those presented in figure 3.1.

these measurements for a delay of 1 μs. By combining all individually captured images, we obtain a representative image of the shock. Note that only half of the low density cavity is visible because of the limited extent of the breakdown plasma created by the second laser.

Complementary to the novel visualisation technique presented above, we visualised the expanding low density cavity, and thereby the propagating shock, using high-speed Schlieren imaging. This technique is sensitive to the first derivative of the density, in the direction normal to a knife edge positioned at the shared focal plane of the 4f lens system used for imaging the side of the toroidal plasma.[12] In figure 3.4 we present these Schlieren images. Note that in the bottom half of the figure, the breakdown plasma has been moved out of sight, to the right of the image, to be able to image the propagating shock at later times.
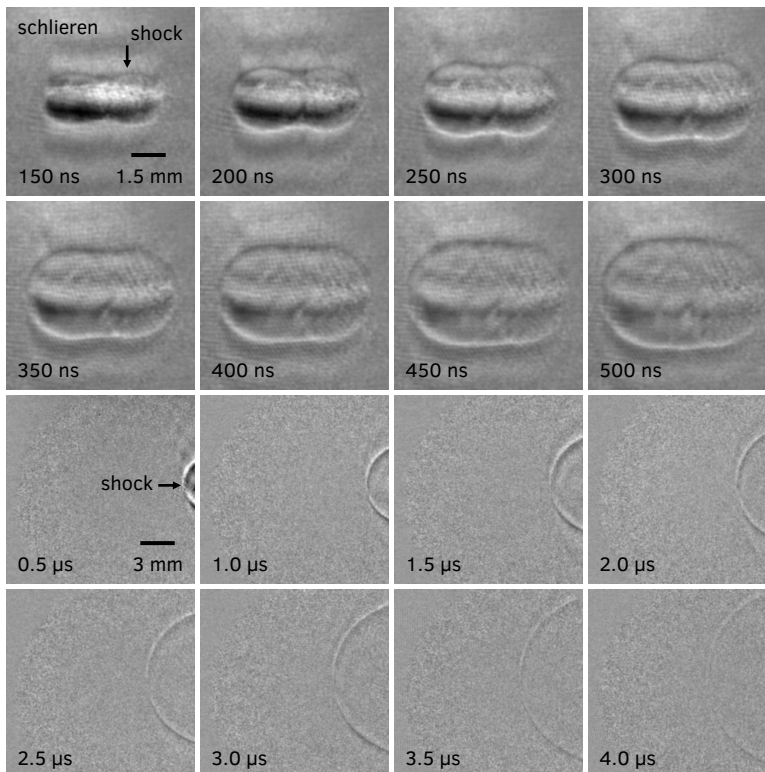
[12] Settles 2001.

Figure 3.4: Propagation of a shock generated by a laser-induced breakdown plasma, visualised using high-speed Schlieren imaging with a helium-neon laser source. Note that in the bottom half of the figure the breakdown plasma has been moved out of sight to the right of the image. The images have been captured at increasing times after the breakdown laser pulse and are corrected for the remaining plasma emission still visible through the Schlieren imaging system (see text for details). This correction is not perfect as is apparent from the structure still visible within the shock. The images are based on recordings captured using similar experimental settings as those presented in figure 3.1.
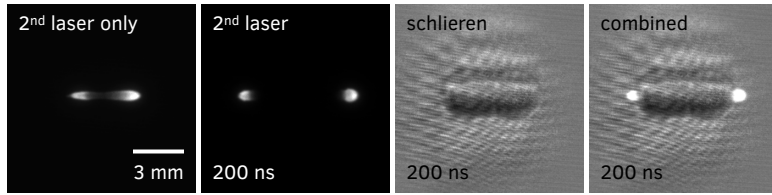
Figure 3.5: Plasma and high-speed Schlieren images have been combined (right) to show that a second laser-induced breakdown plasma (2nd laser) is created on the edge of a shock (schlieren) generated by a laser-induced breakdown plasma created earlier (not shown). Without a previously generated breakdown plasma the second breakdown plasma shows its regular two-lobe structure (2nd laser only).

The presented Schlieren images have been corrected for the remaining plasma emission still visible through the helium-neon laser line filter, by subtracting images that have been captured while the helium-neon laser of the Schlieren imaging system was switched off. This process is not perfect, as is apparent from the structure resembling the two-lobe plasma kernel, still visible within the shock.

We end this section by presenting an experiment where we combine images of a laser-induced breakdown plasma with high-speed Schlieren images of a shock, generated by a laser-induced breakdown plasma created earlier. When we compare the leftmost two images in figure 3.5, obtained respectively with and without the first breakdown plasma present, we observe that the second breakdown plasma is expelled outward. The combined plasma and high-speed Schlieren image shows that the second plasma is expelled outward, exactly to the point where the shock separates the low density cavity from the ambient gas.

3.3 *Mach reflection and laser-induced breakdown plasmas*

When we revisit the plasma kernel images presented in figure 2.26, and the radiant intensity of these images in figure 2.27, we observe that around 54 ns the plasma emission is at its brightest. Precisely at this moment, the plasma kernel exhibits a two-lobe structure consisting of two almost isolated bright plasmas. These two bright lobes are two high pressure and high temperature plasmas, both rapidly expanding and both leading to the formation of a shock. The imprint of these two lobes was already visible in the high-speed Schlieren images presented in figure 3.4, most notably around 250 ns, where we can observe two overlapping spherical shocks.

We reproduced this Schlieren image in figure 3.6. A notable feature that can be observed is a Mach reflection. At a sufficiently oblique

intersection of two shocks, a new third shock is generated, which has a higher strength and which propagates faster than the primary shocks.[13] The two shocks join to form a third shock, the Mach reflection. Because the Mach reflection significantly increases the strength of the shock, it was studied by Reines and Von Neumann to determine the optimum height of burst of an atomic bomb, to provide the greatest possible destructive effect on the ground.[14]

In figure 3.6 we also reproduced, alongside our high-speed Schlieren image of the two interacting shocks, a historical image by Mach et al.,[15] and their resemblance is striking. In their measurements, Mach et al. visualised the interaction of two almost spherical shocks, generated using two electric sparks.

With the obtained insights we revisit the numerical studies on the onset and dynamics of plasma kernels,[16] and reproduce a selection of their simulations in figure 3.7. Although slightly asymmetric, these images also show a striking similarity with our high-speed Schlieren image, and hence with the shock interaction imaged by Mach et al. These simulations show that a Mach reflection indeed represents a stronger and more dense shock, as is noted by the authors,[17] but they have not identified it as a Mach reflection. In a laser-induced breakdown spectroscopy study,[18] a Mach reflection due to the reflection of a shock on a brass surface has been identified.

The fact that a Mach reflection represents a stronger shock, provides

[13] Krehl and Van der Geest 1991.

[14] Krehl and Van der Geest 1991; Glasstone et al. 1977.

[15] Mach et al. 1890; Krehl 2011, p. 97.

[16] Alberti, Munafò, Pantano et al. 2019a; Alberti, Munafò, Pantano et al. 2019b; Alberti, Munafò, Koll et al. 2020.

[17] Alberti, Munafò, Pantano et al. 2019a.

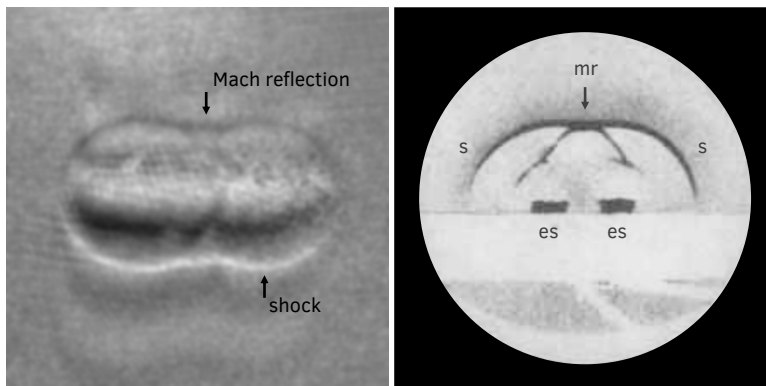[18] Cristoforetti et al. 2006.

Figure 3.6: Mach reflection due to the interaction of two shocks generated by the two-lobe plasma kernel of a single laser-induced breakdown plasma created in atmospheric pressure helium gas. (left, reproduced from figure 3.4) High-speed Schlieren image of a breakdown plasma captured 250 ns after the breakdown laser pulse. (right) The very first ever visualisation by Ernst Mach of the interaction of two shocks and generation of a Mach reflection. Mach et al. generated the two nearly spherical shocks (s) using two electric sparks (es) near a glass plate. The interacting shocks generate a third shock known as a Mach reflection (mr). This image is reproduced from Mach et al. 1890, with permission of John Wiley and Sons. Copyright 1890 Wiley-VCH Verlag.
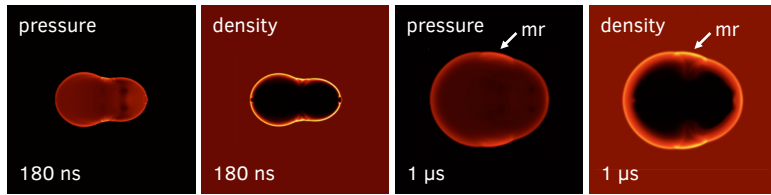
Figure 3.7: Mach reflection visualised by a simulation of the plasma kernel. (left pair) Pressure and density images from early in the development of a plasma kernel. Although slightly asymmetric the images strikingly resemble the high-speed Schlieren image presented in figure 3.6. (right pair) Pressure and density images of a further developed plasma clearly showing the Mach reflection (mr). The images are not to scale. For a numerical interpretation of the images we refer to the original publication. These images are reproduced from Alberti, Munafò, Pantano et al. 2019a, with permission of the American Institute of Aeronautics and Astronautics.

an explanation for the asymmetric fluid flow repleting the low density cavity, which is necessary for our understanding of the development of toroidal plasmas. The higher intensity of the Mach reflection breaks the symmetry, and as a consequence the repleting fluid flow orthogonal to the symmetry axis commences at a later time.

3.4   Conclusion

In this chapter we examined the low density cavity that proved to play a pivotal role in the development of laser-generated toroidal plasmas.

We directly confirmed the existence of this low density cavity using high-speed Schlieren imaging, and presented a novel technique in which we used a second laser-induced breakdown plasma as a probe.

Using this technique, we directly visualised the propagating shock formed by the laser-induced breakdown plasma, and confirmed the existence of the low density cavity in its wake. We found that the motion of the shock is described by a power-law time dependence with an exponent of 0.55 ± 0.02, approximately corresponding to the behaviour of a two-dimensional explosion.

The two-lobe structure of the plasma kernel is found to generate two spherical shocks. A novel interpretation shows that these shocks interact to generate a Mach reflection. The enhanced strength of this Mach reflection provides an explanation for the asymmetric fluid flow necessary for the development of toroidal plasmas.